

Parametric and Nonparametric Methods for Power Line Network Topology Inference

Mohamed Osama Ahmed and Lutz Lampe

Department of Electrical and Computer Engineering, University of British Columbia, Vancouver, Canada
{mohameda, lampe}@ece.ubc.ca

Abstract—Frequency domain reflectometry (FDR) has recently been proposed as a method for inferring the topology of power line communications (PLC) networks. In this paper, we introduce and compare two approaches to process FDR measurements for topology inference. The first approach is based on peak-detection using the inverse Fourier transform of FDR measurements. We refer to this method as the nonparametric method. The second approach is based on a parametric model, which under reasonable assumptions makes Prony-type methods applicable to the problem at hand. The advantages and the limitations of both methods are determined and discussed. Simulation results demonstrate the performance of each method.

I. INTRODUCTION

Power line communications (PLC) [1] is a popular technology whose appeal are cost savings and high penetration through the reuse of existing wiring infrastructure. While most of the attention over the past decade has been given to high-speed in-home PLC, recent research efforts focus on moderate-speed PLC over low-voltage and medium-voltage distribution grids for applications envisaged in Smart Grid. Since the PLC channel is given by the electricity infrastructure, PLC network models follow the physical topology of the power grid. Hence, it is necessary to know the underlying grid topology in order to understand and model topologies of PLC networks (PLNs). Recent work on PLC for Smart Grid has made ad hoc or simplifying assumptions in this regard, since topologies of realistic configurations are not well studied, e.g., [2]–[4]. Moreover, information about power line infrastructure is sometimes not even (accurately) known to electricity utilities. It is therefore desirable to obtain topology information through in-situ measurements, i.e., to perform topology inference. Another important use of such inference would be online grid diagnostics.

In previous work [5], we have proposed a technique for PLN topology inference. This technique is based on distance estimation using frequency domain reflectometry (FDR) measurements. More specifically, it operates in two main steps.

- 1) Estimating the distances of the signal paths in the transmission network.
- 2) Reconstructing the topology by mapping the location information to a network graph.

In this paper, we elaborate on the first step. We point out the limitation of nonparametric location estimation methods,

which perform some sort of peak detection based on FDR measurements and are limited in their resolution. As a solution to this problem, we suggest super-resolution methods, which exploit a parametric model for signal propagation. We show that the location estimation problem is equivalent to estimating the frequencies of complex damped exponential signals from observing their superposition. This problem has been studied for a long time, and different methods have been proposed for estimating the parameters. The Prony method is the classical solution [6]. If the number of parameters to be estimated is unknown, other methods such as the least squares method [7], [8], matrix pencil method [9], or the subspace method [10] can be applied. In this work, we use the subspace method as an example of the parametric methods.

The remainder of this paper is organized as follows. Section II reviews some basic parameters of transmission line theory and explains the FDR principles applied in this work. Then, Section III describes how nonparametric and parametric methods can be used to estimate the distances corresponding to signal propagation paths from FDR measurements. Simulation results illustrating the performances of both methods are presented in Section IV, and conclusions are given in Section V.

II. TOPOLOGY INFERENCE PROBLEM

We adopt the point of view that the problem of topology inference of a PLN can be considered as a channel estimation problem. In this section, we first describe the propagation model applied to describe the channel, which will also be used in Section IV for performance evaluation, and then discuss different approaches to this channel estimation and cast the FDR method into this framework.

A. Propagation Model

Since we consider signal propagation in PLN, a bottom-up parametric propagation model is appropriate. Therefore, we adopt the two-conductor transmission line formalism to approximate the signal propagation over power lines [1, Ch. 2]. Accordingly, we represent transmission lines as two-ports described by its characteristic impedance $Z_0(f)$ and propagation constant $\gamma(f) = \alpha(f) + j\beta(f)$, where $\alpha(f)$ is the attenuation constant, and $\beta(f)$ is the propagation constant, which are functions of the frequency f . Discontinuities, such as branch points, are represented by the reflection and transmission

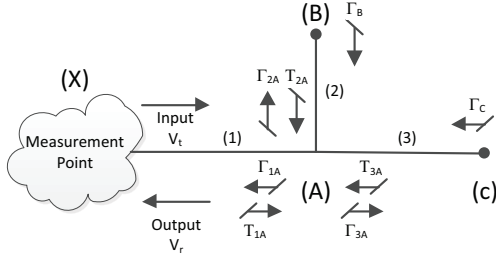


Fig. 1. Example of a PLN topology with 3 points of discontinuity.

coefficients Γ and T , respectively. Γ can be calculated by

$$\Gamma = \frac{Z - Z_0}{Z + Z_0}, \quad (1)$$

and T is given by

$$T = 1 + \Gamma, \quad (2)$$

where Z is the equivalent impedance at the point of discontinuity (the point of reflection).

Then, when a signal propagates through a transmission line, part of the transmitted power is reflected and another part is transmitted at the points of discontinuities. For topology inference, a signal is induced at one point of the PLN and also, via directional coupling, received at the same point. Hence, we can express the channel transfer function between transmitted and received signal as

$$H(f) = \sum_{i=1}^{\infty} A_i(f) e^{-2d_i \gamma(f)}, \quad (3)$$

where d_i and $A_i(f)$ is the distance and the product of the reflection and transmission coefficients for the i th reflection, respectively. We note that the set of d_i does not only include the distances of the discontinuities from the point of measurement, but also distances traveled by signals bouncing between discontinuities.

In (3), the summation is infinite because of these multiple reflections. That is, even though the number of discontinuities is finite, there are infinitely many paths of signal propagation. However, since reflection and transmission as well as propagation along transmission lines lead to power loss of the propagating wave, in practical cases the summation can be limited to a finite number, K , of terms accounting for the significant paths.

Figure 1 shows an example of a PLN with 3 reflection points, labeled A, B, and C, and three branches, numbered 1, 2, and 3. The reflection and transmission coefficients for each reflection point are also indicated in Fig. 1. Denoting, at the measurement point X, the input and output voltage signal as $v_t(t)$ and $v_r(t)$ and their Fourier transforms as $V_t(f)$ and $V_r(f)$, respectively, we have $H(f) = V_r(f)/V_t(f)$, and the channel transfer function is given as in (3). For example, considering the path X-A-B-A-X, the coefficient $A(f)$ for this path is given by $A(f) = T_{1A} \Gamma_B T_{2A}$, and the round trip distance for this path is $d = 2(d_1 + d_2)$.

In [5], we presented an algorithm that given the distances d_i , reconstructs the topology of PLN. Thus, the topology inference problem is reduced to estimating the distances d_i , which can be interpreted as parametric estimation of the channel $H(f)$.

B. Channel Estimation

One approach to find the distances d_i is to send a signal $v_t(t)$ with certain pulse shaping. The received signal $v_r(t)$ is then typically matched filtered and sampled for maximal matched filter output. Considering the frequency-dependent signal distortion, time-frequency methods can be used to design the transmitted signal, and then the information about the reflection points can be extracted using time-frequency analysis methods. In [11], a comparison between different time-frequency analysis methods is presented. The time-frequency methods can enhance the resolution as will be discussed later. Another approach is to measure $H(f)$ at discrete frequency points, one at a time, and then infer on d_i . This latter approach is used in what is called frequency domain reflectometry (FDR).

C. FDR Overview

FDR is a technique that was proposed for fault detection in cables, cf. e.g. [12]–[16]. In FDR the transmission line is excited with a sinusoidal signal of frequency f_0 , and amplitude A . That is,

$$v_t(t) = A \cos(2\pi f_0 t). \quad (4)$$

The transmitted signal is reflected from the the points of discontinuities at distance d_i from the measurement point. Since $v_t(t)$ is a sinusoid, we have for the reflected signal

$$v_r(t) = \frac{A}{2} (H(f_0) e^{j2\pi f_0 t} + H(-f_0) e^{-j2\pi f_0 t}), \quad (5)$$

and using (3), the total reflected signal can be written as

$$v_r(t) = A \sum_{i=1}^{\infty} |A_i(f_0)| e^{-2\alpha(f_0) d_i} \times \cos(2\pi f_0 t - 2\beta(f_0) d_i + \angle A_i(f_0)), \quad (6)$$

where $A_i(f) = |A_i(f)| e^{j\angle A_i(f)}$. The reflected signal is correlated with the transmitted signal and the output is passed through a low pass filter for coherent detection. The output of the low pass filter is called the trace $Y(f_0)$ and given by [14]

$$Y(f_0) = \frac{1}{T} \int_0^T v_r(t) v_t(t) dt \quad (7)$$

$$= \frac{A}{2} \sum_{i=1}^{\infty} |A_i(f_0)| e^{-2\alpha(f_0) d_i} \times \cos(2\beta(f_0) d_i - \angle A_i(f_0)) \quad (8)$$

$$= \frac{A}{2} (H(f_0) + H(-f_0)), \quad (9)$$

where T should be multiple of $1/f_0$. Relation (9) shows that FDR can also be understood as channel estimation (or sounding), and the complex transfer function would be obtained by also sending a 90° shifted signal.

The trace is measured for a certain frequency range $f_{\min} \leq f \leq f_{\max}$, with a certain step size Δf . In case of low losses¹, β can be approximated as a linear function of f given by $\beta = 2\pi f\sqrt{LC}$, where L and C are the inductance and the capacitance of the transmission line per unit length. Hence, the propagation velocity is $v = \frac{1}{\sqrt{LC}}$. In this case, the trace $Y(f)$ at frequency f can then be expressed as

$$Y(f) = \frac{A}{2} \sum_{i=1}^{\infty} |A_i(f)| e^{-2\alpha(f)d_i} \cos\left(4\pi f\sqrt{LC}d_i - \angle A_i(f)\right). \quad (10)$$

Based on this trace, the distances d_i can be determined as will be discussed in the following.

III. DISTANCE MEASUREMENT

As mentioned above, the PLN topology inference problem is reduced to obtaining the distances $2d_i$ traveled by PLC signals in the PLN. In the following, we first present two approaches, namely parametric and nonparametric, for this purpose.

A. Nonparametric Methods

We refer to nonparametric methods as methods that directly work on the trace $Y(f)$ of FDR and do not take the specific form (3) of the channel transfer function $H(f)$ into account. More specifically, taking the Inverse Fourier Transform (IFT) of $Y(f)$ with respect to the frequency f , the signal is transformed to the correlation $y(t)$ in the time domain. As can be inferred from (10), $y(t)$ will have peaks at $t_i = 2\sqrt{LC}d_i$, and thus the length of this signal path can be calculated as $vt_i = 2d_i$.

The nonparametric methods estimate location of the peaks in the correlation signal $y(t)$. The performance of these methods is limited by the time-frequency uncertainty. In order to enhance the resolution in the time domain, more measurement bandwidth $B = f_{\max} - f_{\min}$ is required. The time resolution can be approximated by

$$\Delta t \approx \frac{1}{B}. \quad (11)$$

Thus, there is a minimum distance $\Delta d_{\min} = v\Delta t$ below which two reflection points cannot be separated. The distance resolution can be approximated by

$$\Delta d_{\min} \approx \frac{1}{(f_{\max} - f_{\min})\sqrt{LC}}. \quad (12)$$

However, resolution is not limited by the finite bandwidth only. The path gains $A_i(f)$ as well as the attenuation term $\alpha(f)$ are frequency dependent, which leads to a broadening of the peaks in $y(t)$, which is the ‘‘spectral’’ leakage problem. The dilemma is that increasing the bandwidth pronounces the leakage through frequency selectivity of $A_i(f)$ and $\alpha(f)$. Hence, the resolution of nonparametric methods is intrinsically limited.

¹If this is not true, then the analysis can be extended to the general case by rescaling the frequency axis properly as discussed in [14].

B. Parametric Methods

Parametric methods overcome the resolution limitation of their nonparametric counterparts, which is why they are also referred to as super-resolution methods. The reason for this seeming advantage is the reliance on a signal model. For the problem considered here, we make the assumption that $\alpha(f)$ and $\beta(f)$ are (well approximated as) linear functions of the frequency, i.e., $\alpha(f) = af$, $\beta(f) = bf$. We further assume that the coefficients $A_i(f)$ are constant over the frequency measurement range. This is not as strong an assumption as it may appear at first glance, as the frequency range can be quite narrow compared to the nonparametric case. Furthermore, extensions to frequency-selective $A_i(f)$ are possible, but not considered here for clarity. Using these assumptions, equation (3) can be rewritten as

$$H(f) = \sum_{i=1}^K A_i e^{-2d_i af} e^{-j2d_i bf}, \quad (13)$$

where we truncated the sum to K terms corresponding to the dominating (and thus measurable) paths. If measurements of the channel transfer function (using, for example, FDR or any other scheme such as multicarrier transmission with cyclic prefix) are recorded for N discrete frequency points f_k uniformly spaced with Δf , i.e. $f_k = f_{\min} + k\Delta f$, $k = 0, 1, \dots, N-1$, then we have a set of measurement points

$$\begin{aligned} H_k &\triangleq H(f_k) \\ &= \sum_{i=1}^K A_i e^{-2f_{\min}(a+jb)d_i} e^{-2k\Delta f(a+jb)d_i} \\ &\triangleq \sum_{i=1}^K B_i e^{-2k\Delta f(a+jb)d_i} \end{aligned} \quad (14) \quad (15)$$

where we introduced $B_i = A_i e^{-2f_{\min}(a+jb)d_i}$.

Given H_k , $k = 0, 1, \dots, N-1$, and the representation (15), the estimation of d_i is equivalent to the well known problem of spectral estimation of complex damped exponentials. This problem can be solved using Prony’s method [6]. The Prony method converts this nonlinear problem into three linear problems as follows:

- 1) Using H_k , $k = 0, 1, \dots, N-1$, construct a linear prediction equation with unknown coefficients. The coefficients can then be determined if the number of measurement points N satisfies $N \geq 2K$.
- 2) Determine the exponents $(-2\Delta f(a+jb)d_i)$ in our case) from the roots of the characteristic polynomial formed by the prediction coefficients.
- 3) Calculate the amplitudes B_i by solving a Vandermonde system of equations.

Since the number of discontinuities is not known a priori, K is unknown. Different methods have been proposed for this case, e.g. the SVD-Prony method [17]. Other methods can be used to solve this problem, including

- iterative maximum likelihood or least squares methods [7], [8],

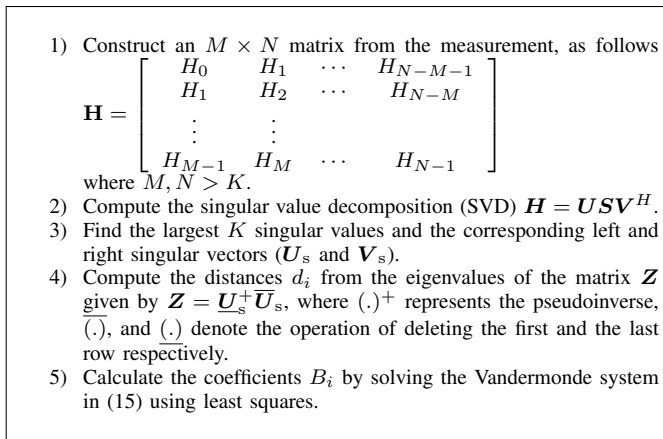


Fig. 2. Subspace algorithm.

- polynomial or linear prediction methods [17]–[19],
- matrix pencil method [9],
- subspace method [10].

In our experiments, we tried a number of different methods for the inference problem at hand. The subspace method showed better results for large K . Although all of the spectral estimation methods should recover the parameters correctly in the noiseless case, some methods are more sensitive to limited numerical resolution, which becomes an issue for larger K . In Fig. 2, we summarize the the main steps of the subspace method. We refer the reader to [10] and [20] for the mathematical details involved in deriving the subspace algorithm.

C. Maximum Detectable Distance

Since the measurements are taken for discrete frequency points, this is equivalent to sampling the trace $Y(f)$ (or the channel transfer function $H(f)$) with interval Δf . Thus, the correlation $y(t)$ will be periodic. Δf should be chosen in order to prevent aliasing. If the maximum distance to be detected is d_{\max} (corresponding in time to $t_{\max} = 2d_{\max}/v$), then the Nyquist sampling criterion states

$$\frac{1}{\Delta f} \geq 2t_{\max}, \quad (16)$$

and thus Δf must satisfy

$$\Delta f \leq \frac{1}{4d_{\max}\sqrt{LC}}. \quad (17)$$

IV. RESULTS AND DISCUSSION

In this section, we present numerical results to compare the nonparametric and parametric approaches for distance estimation.

A. Simple Example

In order to demonstrate the resolution limitation of the nonparametric method, we start with the following simple example. Consider a simple transfer function $H(f_k)$ given by

$$H(f_k) = B_1 e^{-d_1 \gamma(f_k)} + B_2 e^{-d_2 \gamma(f_k)}, \quad (18)$$

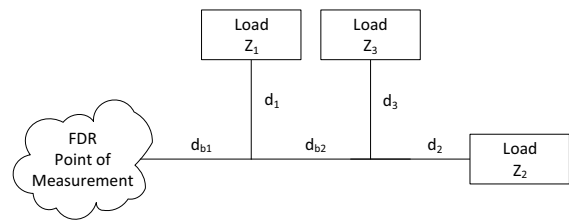


Fig. 3. Topology used for numerical results.

where $B_1 = B_2 = 1/2$, $\gamma(f_k) = (1.5 \times 10^{-9} + j4.2 \times 10^{-8})f_k$, and $d_1 = 100$ m, and $d_2 = 100.1$ m. So the model order is $K = 2$. For a bandwidth of 500 kHz, the resolution for the nonparametric method is $\Delta d_{\min} \approx 300$ m. So the nonparametric method could find only one peak at $d = 100$ m. While the parametric method could detect the two reflections accurately with such small bandwidth (using $\Delta f = 0.2$ kHz).

B. Network Parameters

Moving on to more practical cases, Figure 3 shows the sample topology that was used to generate $H(f)$ and $Y(f)$. The frequency range for the measurement was chosen from $f_{\min} = 50$ kHz to different values of f_{\max} , as will be specified for each experiment. The transmission line parameters for the line pieces in Figure 3 are those for NAYY150SE power line cables adopted from [1, Ch. 2.3]. The distances are $d_{b1} = 200$ m, $d_{b2} = 1.3d_{b1}$, $d_1 = 4.1d_{b1}$, $d_2 = 15d_{b1}$, and $d_3 = 5.25d_{b1}$. The loads were chosen with the following reflection coefficients: $\Gamma_1 = 1/4$, $\Gamma_2 = 1/5$, and $\Gamma_3 = 1/8$. As an estimate for the number of signal paths, let us assume that the maximum number of reflections per branch is three. Then, the total number of reflected signal paths would be $K = 196$.

C. Setup of Methods

For the nonparametric peak-detection method, in [14], conditions on the minimum value of the peaks, and the values of the first derivative were imposed on the local maxima to distinguish between the true peaks from those due to sidelobes. We chose the values for these thresholds empirically. The peaks from sidelobes may cause false alarms.

We tested the following five scenarios.

- 1) Case 1: $f_{\max} = 950$ kHz, $\Delta f = 1$ kHz, and linear $\alpha = 1.5 \times 10^{-9} \text{sm}^{-1} \times f$.
- 2) Case 2: $f_{\max} = 950$ kHz, $\Delta f = 1$ kHz, and α calculated using transmission line parameters as described in [1, Ch. 2.3] for NAYY150SE power line cables (α for this case has a square root dependency on the frequency).
- 3) Case 3: $f_{\max} = 2.5$ MHz, $\Delta f = 2$ kHz, and linear $\alpha = 1.5 \times 10^{-9} \text{sm}^{-1} \times f$.
- 4) Case 4: $f_{\max} = 2.5$ MHz, $\Delta f = 2$ kHz, and α as in case 2.
- 5) Case 5: $f_{\max} = 500$ kHz, $\Delta f = 0.2$ kHz, and α as in case 2.

The above cases were chosen to highlight the effect of the bandwidth and the approximation of linear $\alpha(f)$ on the performance of the methods, respectively.

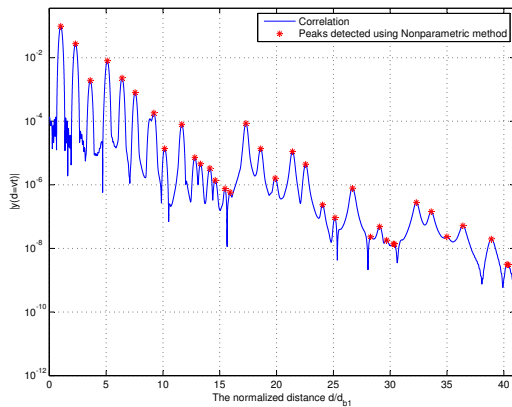


Fig. 4. Illustration of peak detection using nonparametric method. The correlation $|y(d = vt)|$ as function of the normalized distance d .

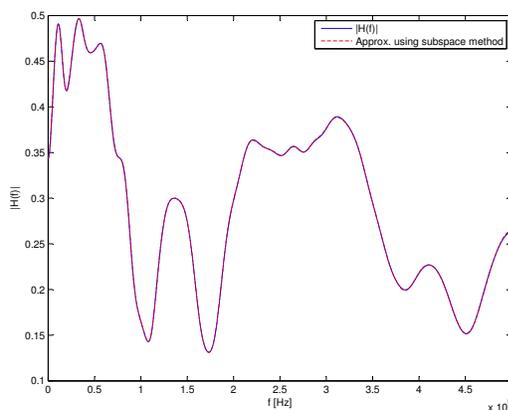


Fig. 5. Illustration of the approximation of the magnitude transfer function $|H(f)|$ using the subspace method.

As an example, Figure 4 shows the magnitude correlation $|y(d = vt)|$ as function of distance d and the detected peaks using the nonparametric method for case 4. We note that some of the detected peaks are actually due to sidelobes and thus cause false alarms. Figure 5 shows the magnitude transfer function $|H(f)|$ and its approximation using equation (15). It can be seen that the subspace method provides an excellent approximation of $|H(f)|$ using a superposition of damped complex exponentials.

D. Performance and Discussion

An objective performance evaluation for the location estimation is fairly complicated, as both detecting a signal path and accuracy matter. We therefore list in Tables I, II and III the true and estimated distances for parametric and nonparametric method and the different cases, respectively. Note that missed locations are indicated by “x”. In Table I, the magnitude of the coefficient of each exponential component $|C_i|$ is presented, where $C_i = |A_i|e^{-2\alpha(f)d_i}$ and $\bar{\alpha}(f)$ is the mean of $\alpha(f)$ over the considered frequency range. C_i can be viewed as the weight of the i th signal path. As C_i increases, it should be easier to detect the corresponding component. For some

reflections, C_i can be zero due to multiple paths having the same distance and interfering destructively. In our example, this happened for $d = 7.7d_{b1}$, $10.5d_{b1}$, and $12.95d_{b1}$. In this case, it is impossible to detect such paths, and the algorithm for topology reconstruction should consider this possibility. In Table I the magnitude of C_i is computed for case 1.

The results in Tables I and II show that if $\alpha(f)$ is not linear in f , some performance degradation for the parametric method results. But overall this is not dramatic. For the parametric method, some signal paths are not detected. This indicates that different parameter sets for (15) lead to only slightly different approximations of $H(f)$. Optimizing the sampling interval as in [21] could mitigate this problem. Another improvement could be obtained from successively removing the effect of located reflections. Our experiments showed that by subtracting the first exponential term from the measured $H(f)$ (with $d = d_{b1}$), some of the missing paths could be detected.

For the nonparametric method, we observe from Table III that the signal bandwidth is decisive to properly estimate the correct distances. For small bandwidth of 500 kHz (Case 5), the nonparametric fails, while the parametric could find some signal paths. Comparing the results from Tables I, II and III, we observe that the parametric method can achieve the same accuracy of distance estimation with much smaller bandwidth. This illustrates the benefit of the super-resolution approach.

It is important to note that the nonparametric method is limited by the resolution-bandwidth relation. While the parametric methods are limited by the model order K . As K increases, the accuracy of the model decreases due to the numerical sensitivity of the parametric method. Increasing the bandwidth helps decrease the numerical error. We are currently working on ways of improving numerical robustness.

V. CONCLUSION

In this paper, we have extended our previous work on inference of a PLN topology. We have focused on the first step of the inference, which is the distance estimation of signal paths. Considering this problem as an instance of channel estimation, a parametric methodology has been derived. In particular, parameter estimation methods known from spectral estimation become applicable. These methods overcome the problem of the nonparametric peak-detection approach, whose resolution is limited by the signal bandwidth. This has been confirmed through simulation tests.

REFERENCES

- [1] H. Ferreira, L. Lampe, J. Newbury, and T.G. Swart (Editors), *Power Line Communications: Theory and Applications for Narrowband and Broadband Communications over Power Lines*. John Wiley & Sons, Jun. 2010.
- [2] G. Srinivasa Prasanna, A. Lakshmi, S. Sumanth, V. Simha, J. Bapat, and G. Koomullil, “Data communication over the smart grid,” in *IEEE International Symposium on Power Line Communications and Its Applications (ISPLC)*, Mar.-Apr. 2009, pp. 273–279.
- [3] G. Bumiller, L. Lampe, and H. Hrasnica, “Power line communications for large-scale control and automation systems,” *IEEE Commun. Mag.*, vol. 48, no. 4, pp. 106–113, Apr. 2010.

TABLE I
NORMALIZED ACTUAL AND DETECTED PATHS (d/d_{b1}) FOR THE
PARAMETRIC METHOD.

C_i (Case 1)	Actual Distance	Parametric (Case 1)	Parametric (Case 2)
0.24	1	1	1
0.072	2.3	2.3	2.3
0.005	3.6	3.6	3.61
3.8×10^{-4}	4.9	4.9	x
0.022	5.1	5.1	5.1
0.0065	6.4	6.4	6.4
0.0023	7.55	7.55	7.54
0	7.7	x	x
3.3×10^{-4}	8.85	8.86	x
3.54×10^{-4}	9	x	8.99
5×10^{-4}	9.2	9.21	9.3
3.69×10^{-5}	10.15	10.16	10.25
0	10.5	x	x
2.1×10^{-4}	11.65	11.66	11.65
3.3×10^{-5}	11.8	x	x
1.8×10^{-5}	12.8	x	x
0	12.95	x	x
1.6×10^{-6}	13.1	12.99	x
1.15×10^{-5}	13.3	x	13.3
7.9×10^{-6}	14.1	x	14.09
3.36×10^{-6}	14.25	14.19	x

TABLE II
NORMALIZED ACTUAL AND DETECTED PATHS (d/d_{b1}) FOR THE
PARAMETRIC METHOD.

Actual Distance	Parametric (Case 3)	Parametric (Case 4)	Parametric (Case 5)
1	1	1	1
2.3	2.3	2.3	2.3
3.6	3.6	3.6	3.62
4.9	4.9	4.78	x
5.1	5.1	5.09	5.1
6.4	6.4	6.4	6.39
7.55	7.55	7.55	7.54
7.7	x	x	x
8.85	8.85	8.86	x
9	x	8.97	9
9.2	9.2	9.18	9.16
10.15	10.15	10.13	x
10.5	x	x	x
11.65	11.65	11.66	11.7
11.8	11.8	11.71	x
12.8	12.8	12.81	x
12.95	x	x	x
13.1	13.2	13.3	x
13.3	13.3	x	13.45
14.1	14.06	x	x
14.25	14.19	14.2	x

[4] M. Biagi and L. Lampe, "Location assisted routing techniques for power line communication in smart grids," in *IEEE International Conference on Smart Grid Communications (SmartGridComm)*, Oct. 2010.

[5] M. O. Ahmed and L. Lampe, "Power line network topology inference using frequency domain reflectometry," in *submitted to the IEEE International Communications Conference (ICC)*, Ottawa, Canada, Jun. 2012.

[6] R. Prony, "Essai experimental et analytique," *Journial de L'ecole Polytechnique*, vol. 2, pp. 24 – 76, 1795.

[7] Y. Bresler and A. Macovski, "Exact maximum likelihood parameter estimation of superimposed exponential signals in noise," *IEEE Trans. Acoust., Speech, Signal Process.*, vol. 34, no. 5, pp. 1081–1089, 1986.

[8] R. Kumaresan, L. Scharf, and A. Shaw, "An algorithm for pole-zero

TABLE III
NORMALIZED ACTUAL AND DETECTED PATHS (d/d_{b1}) FOR THE
NONPARAMETRIC METHOD.

Actual Distance	Nonparametric (Case 2)	Nonparametric (Case 4)	Nonparametric (Case 5)
1	1.04	1	1.04
2.3	2.3	2.3	x
3.6	3.61	3.6	x
4.9	x	x	x
5.1	5.1	5.1	5.12
6.4	6.4	6.4	x
7.55	7.56	7.55	x
7.7	x	x	x
8.85	x	8.86	x
9	x	x	x
9.2	9.14	9.19	x
10.15	x	10.15	10.1
10.5	x	x	x
11.65	11.63	11.65	11.58
11.8	x	x	x
12.8	12.87	12.8	x
12.95	x	x	x
13.1	x	x	x
13.3	x	13.3	x
14.1	14.06	14.11	x
14.25	x	x	x

modeling and spectral analysis," *IEEE Trans. Acoust., Speech, Signal Process.*, vol. 34, no. 3, pp. 637–640, 1986.

[9] Y. Hua and T. Sarkar, "Matrix pencil method for estimating parameters of exponentially damped/undamped sinusoids in noise," *IEEE Trans. Acoust., Speech, Signal Process.*, vol. 38, no. 5, pp. 814–824, 1990.

[10] I. Maravic and M. Vetterli, "Sampling and reconstruction of signals with finite rate of innovation in the presence of noise," *IEEE Trans. Signal Process.*, vol. 53, no. 8, pp. 2788 – 2805, Aug. 2005.

[11] Y. Shin, "Theory and application of time-frequency analysis to transient phenomena in electric power and other physical systems," Ph.D. dissertation, University of Texas at Austin, 2004.

[12] B. Celaya and D. Dodds, "Single-ended DSL line tester," in *Canadian Conf. on Electr. and Comp. Eng. (CCECE)*, vol. 4, May 2004, pp. 2155 – 2158.

[13] D. E. Dodds, M. Shafique, and B. Celaya, "TDR and FDR identification of bad splices in telephone cables," in *Canadian Conf. on Electr. and Comp. Eng. (CCECE)*, May 2006, pp. 838 – 841.

[14] B. de la Torre, "DSL line tester using wideband frequency domain reflectometry," Master's thesis, University of Saskatchewan, 2004.

[15] D. Dodds and B. Celaya, "Locating water ingress in telephone cables using frequency domain reflectometry," in *Canadian Conf. on Electr. and Comp. Eng. (CCECE)*, May 2005, pp. 324 – 327.

[16] D. Dodds, "Single-ended FDR to locate and specifically identify DSL loop impairments," in *IEEE Intl. Conf. Commun. (ICC)*, Jun. 2007, pp. 6413 – 6418.

[17] R. Kumaresan and D. Tufts, "Estimating the parameters of exponentially damped sinusoids and pole-zero modeling in noise," *IEEE Trans. Acoust., Speech, Signal Process.*, vol. 30, no. 6, pp. 833 – 840, Dec. 1982.

[18] D. Tufts and R. Kumaresan, "Estimation of frequencies of multiple sinusoids: Making linear prediction perform like maximum likelihood," *Proc. IEEE*, vol. 70, no. 9, pp. 975 – 989, Sep. 1982.

[19] M. Rahman and K.-B. Yu, "Total least squares approach for frequency estimation using linear prediction," *IEEE Trans. Acoust., Speech, Signal Process.*, vol. 35, no. 10, pp. 1440 – 1454, Oct. 1987.

[20] I. Maravic, "Sampling methods for parametric non-bandlimited signals: extensions and applications," Ph.D. dissertation, École Polytechnique Fédérale de Lausanne (EPFL), 2004.

[21] J.-H. Lee and H.-T. Kim, "Selection of sampling interval for least squares prony method," *IEE Electronics Letters*, vol. 41, no. 1, pp. 47 – 49, Jan. 2005.